



Contents lists available at ScienceDirect

LWT

journal homepage: www.elsevier.com/locate/lwt

Feasibility of water-to-ethanol solvent exchange combined with supercritical CO₂ drying to turn pea waste into food powders with target technological and sensory properties

Lara Manzocco^a, Lorenzo Barozzi^a, Stella Plazzotta^{a,*}, Yanjun Sun^b, Song Miao^b,
Sonia Calligaris^a

^a Department of Agricultural, Food, Environmental and Animal Sciences, University of Udine, Via Sondrio 2/a, 33100, Udine, Italy

^b Teagasc Food Research Centre, Moorepark, Fermoy, Co. Cork, P61 C996, Ireland

ARTICLE INFO

Keywords:

Supercritical carbon dioxide
Fiber
Protein
Food waste valorization
Water and oil loading

ABSTRACT

Ethanol solvent exchange combined with supercritical-CO₂-drying (SE + SCD), was applied to upcycle sub-standard peas generated by industrial processing into food powders with target technological and sensory properties. Control powders were produced by traditional air- (AD) and freeze- (FD) drying. SE + SCD promoted carbohydrate and lipid leaching, resulting in a pea powder with protein (32 g/100 g) and fiber content (30 g/100 g) higher than that of AD and FD powders. SE + SCD also caused conformational changes in hemicellulose and partial protein denaturation, as detected by FTIR. Compared to AD and FD powders, SE + SCD one was colourless and more porous, as indicated by the low density (0.16 g cm⁻³) and SEM microstructure. The open-pore structure of SE + SCD powder also accounted for higher water (5.2 g water/g powder) and oil (4.7 g oil/g powder) holding capability. Sensory analysis revealed that SE + SCD produced a flavourless powder, with no vegetable sensory notes.

1. Introduction

Fruit and vegetable processing generates tons of waste (fruit and vegetable waste, FVW), which are currently mainly subjected to anaerobic digestion, while part of them is landfilled, with high disposal costs and environmental impact. Besides, these waste management strategies result in the loss of valuable FVW compounds, including proteins, fibers, and bioactives. Therefore, the development of technological interventions for the upcycling of FVW into novel ingredients is highly demanded to increase the sustainability of the fruit and vegetable food industry (Esparza, Jiménez-Moreno, Bimbela, Ancín-Azpilicueta, & Gandía, 2020).

The integral conversion of FVW into food powders by drying would well fit into this novel waste management approach, allowing a critical biomass to be converted into a shelf-stable ingredient without any residual waste. Drying of food matrices can be performed by applying different technologies. Conventional air-drying (AD) exploits a hot air

flow to induce water evaporation. For instance, AD in the 65–90 °C temperature range has been applied to produce powdered ingredients from fruit and vegetable wastes (Kaveh, Abbaspour-Gilandeh, Fatemi, & Chen, 2021). Although presenting limited investment costs, AD can induce undesired phenomena (e.g., non-enzymatic browning), leading to brown powders with impaired sensory and nutritional properties. AD also causes intense shrinkage and hardening of the plant tissue, which decreases powder technological functionality (e.g., poor rehydration ability) (Kaveh et al., 2021; Strumillo & Adamiec, 1996). On the opposite, freeze-drying (FD) is based on low-temperature water removal by sublimation, which leads to porous powders with high nutritional quality. Nevertheless, when applied to vegetable powder production, the ability of FD to preserve the original material composition (Jakubczyk & Jaskulska, 2021) results in powders presenting a pronounced sensory profile, which would hardly fit in the formulation of most foods, where vegetable sensory notes are not acceptable (Roland et al., 2017).

Abbreviations: AD, air-drying; FD, freeze-drying; SE, solvent exchange; SCD, supercritical-CO₂-drying; SE + SCD, solvent exchange combined with supercritical-CO₂-drying; FVW, fruit and vegetable waste; WHC, water holding capacity; OHC, oil holding capacity; FTIR, Fourier transform infrared spectroscopy; SEM, scanning electron microscope.

* Corresponding author.

E-mail address: stella.plazzotta@uniud.it (S. Plazzotta).

<https://doi.org/10.1016/j.lwt.2024.115778>

Received 30 September 2023; Received in revised form 8 January 2024; Accepted 19 January 2024

Available online 25 January 2024

0023-6438/© 2024 The Authors. Published by Elsevier Ltd. This is an open access article under the CC BY license (<http://creativecommons.org/licenses/by/4.0/>).

Supercritical-CO₂-drying (SCD) has been proposed as a promising alternative to traditional drying processes (Pravallika, Chakraborty, & Singhal, 2023). In this case, water is removed from the food matrix by exposing the product to a flow of supercritical CO₂, which solubilizes water without formation of vapour-liquid interfaces, leading to products with higher porosity than FD ones (Brown, Fryer, Norton, Bakalis, & Bridson, 2008; García-González, Camino-Rey, Alnaief, Zetzl, & Smirnova, 2012). Also, SCD operates under mild temperatures (<50 °C) and pressures (<20 MPa), which prevents degradation reactions and guarantees high retention of bioactive compounds (Michelino, Zambon, Vizzotto, Cozzi, & Spilimbergo, 2018). Nevertheless, food SCD usually requires long drying times since water is scarcely soluble in the apolar supercritical CO₂. Thus, an additional polar cosolvent (i.e., ethanol) can be used to increase water solubility (Vatai, Škerget, & Knez, 2009; Zheng, Tian, Ye, Zhou, & Zhao, 2020). This can be achieved by continuously introducing in the SCD reactor a proper amount of ethanol (Brown et al., 2008). Alternatively, a water-to-ethanol solvent exchange procedure (SE) can be applied prior to SCD (SE + SCD). In this case, water in the food sample is substituted with ethanol, which is then quickly removed by supercritical CO₂ (Plazzotta, Calligaris, & Manzocco, 2018a; 2018b). The use of ethanol might provide the additional advantage of removing, besides water, a number of compounds (e.g., pigments, flavours) responsible for the typical sensory properties of the food matrix (Brown et al., 2008; Plazzotta et al., 2018a; Plazzotta et al., 2018a; Vatansever, Whitney Ohm, Simsek, & Hall, 2021). In this regard, supercritical process has been recently proven to remove off-flavours and oxidation-prone fatty acids from yellow pea flour (Vatansever, Rao, & Hall, 2020). Similarly, the SE + SCD process applied to lettuce waste resulted in a colourless and tasteless dried powder (Plazzotta et al., 2018a; Plazzotta et al., 2018a).

SE + SCD process is associated with significant polarity changes from the aqueous vegetable matrix to the ethanol-CO₂ environment. The latter might strongly affect the conformation of the hydrophilic compounds of the plant matrix as well as their interaction. In this regard, starch was reported to undergo intra-molecular rearrangements, driven by hydrophilic interactions (Vatansever, Whitney, Ohm, Simsek, & Hall, 2021); similarly, the process promoted protein denaturation with exposure of hydrophobic residues (Ganesan et al., 2018). Such physical and chemical changes have been recently shown to improve the technological properties, of dried vegetables, i.e., the physical and chemical properties affecting the behavior of food ingredients during storage, processing, preparation and consumption, such as solubility, water and oil holding capacity (Kumar et al., 2022; Wouters, Rombouts, Fierens, Brijs, & Delcour, 2016). For instance, carrots subjected to ethanol-assisted SCD displayed a higher rehydration attitude than the corresponding AD sample in the study of Brown et al. (2008). Plazzotta et al. (2018a) reported that lettuce powders obtained by SE + SCD presented an impressive ability to upload both water and oil. In addition, SCD vegetables are expected to present higher microbial stability than AD and FD ones, due to the antimicrobial effect of the SCD process, as demonstrated on different vegetable materials, including strawberries and apples (Zambon, Zulli, Boldrin, & Spilimbergo, 2022; Zambon, Zulli, Boldrin, & Spilimbergo, 2021). Although the high investment and running costs, and the need for highly specialized know-how strongly limit the wide diffusion of SCD technology, if properly combined with ethanol SE, this technology could be applied to obtain powder ingredients with tailored technological and sensory properties. In the meantime, recycling pathways for both CO₂ and ethanol can be implemented to increase process sustainability (Viganó, Machado, & Martínez, 2015). These process adjustments could contribute to further facilitating the diffusion of this technology, beyond its few current applications at the industrial level.

Green peas are among the commodities that could take advantage of the application of SE + SCD. This is one of the most important crops grown across the World with yearly production exceeding 35 million tons (Tassoni et al., 2020). In the EU, about 1.2 million tons of green

peas are processed yearly, with Italy being the 7th main producer (FAOSTAT, 2021). Today, the demand for these pulses is increasing with forecasted growth in the EU Market at a CAGR of 8.27 % during the period 2020–2025. Additionally, pea transformation is particularly challenging in terms of waste management. Pea processing is in fact concentrated over two months (April–May), during which tons of waste are generated. Peas generally reach the processing site without leaves, vines, and pods and are quickly submitted to cleaning and grading operations, which separate standard peas from substandard ones (yellowish, damaged, stained, or low dimension peas). The latter represent up to 15 % of the overall processed peas, accounting for 0.135 million tons/year of waste only in the EU. Although substandard peas are rich in proteins (5 g/100 g of fresh weight, fw), carbohydrates (14 g/100 g fw) and fibers (5 g/100 g fw), presenting a composition similar to that of the fresh product (USDA, 2015), they are usually subjected to anaerobic digestion (Zia, Ahmed, & Kumar, 2022). Upcycling pea waste into food ingredients is thus a key strategy to increase the sustainability of the pea supply chain. This seems particularly urgent in view of the current plant-protein transition, accounting for an increasing market demand for pea-based products (Akharume, Aluko, & Adedeji, 2021), which is nowadays causing a reduced availability of peas worldwide. To our knowledge, literature data mainly focused on the upcycling of land pea wastes (e.g., pods, vines) (Pooja et al., 2023), while no information has been reported to date on substandard pea recovery.

The present work aimed to investigate the possibility of upcycling industrially generated pea waste, by turning it into dried powders via SE + SCD. The powders were analyzed for their chemical (composition, FTIR) and physical (colour, density, granulometry, SEM microstructure) properties, as well as for interaction with water and oil (wettability, solubility, water and oil holding capacity), and sensory properties. Control powders were produced with traditional AD and FD technologies. The obtained results highlight the potentiality of pea waste powders obtained by SE + SCD as sustainable food ingredients with tailored functionalities.

2. Materials and methods

2.1. Preparation of green pea powders

Substandard fresh green peas were collected in Conserve Italia (Pomposa, Italy), one of the largest EU companies engaged in fruit and vegetable processing, based in Italy. During the pea campaign, over 1500 kg of peas are processed daily. To guarantee the collection of a representative sample, about 25 kg of substandard peas were collected during the selection phase of canned pea production. Vegetable residues and insects were removed and the peas were blanched in water (90 °C, 1 min), cooled in an ice bath (5 min), frozen at –18 °C with a blast-freezer (AOFPS061, Electrolux, Pordenone, Italia), and packed into 1 kg-capacity pouches. Samples were maintained at –18 °C until use, when they were thawed at 4 °C overnight (REX71FR, Electrolux, Pordenone, Italia) and ground for 2 min with a domestic grinder (Type HF800, Moulinex-Greup SEB, Mayenne, France). Ground peas were then subjected to air-drying (AD), freeze-drying (FD) or water-to-ethanol solvent exchange followed by supercritical-carbon dioxide drying (SE + SCD).

For AD, ground peas were distributed on a perforated tray in thin layers and dried at 50 ± 0.5 °C in an air-drying oven (AOS101GTD1, Electrolux, Pordenone, Italy) until constant weight upon three consecutive measures. For FD, ground peas were frozen at –18 °C with a blast-freezer and freeze-dried for 96 h at 20 kPa by using a Christ freeze-drier (Epsilon 2–4 LSCplus, Martin Chirst, Osterode am Harz, Germany). For SE + SCD, ground peas were immersed for 24 h in a 1:8 (w/w) ratio in ethanol (VWR International, Rosny-sous-Bois, France). This procedure was repeated twice. During this time, water was progressively removed from pea matrix, as indicated by monitoring the decrease in the alcoholic degree of the ethanol solution by a lab-alcoholmeter (Alcolyzer plus, Anton Paar, Graz, Austria). Ethanol was then removed by using the

SCD plant developed at the Department of Agricultural, Food, Environmental and Animal Sciences (University of Udine). The plant was furnished by AEROGEX UG Haftungsbeschränkt (Hamburg, Germany) and consists of a pressure vessel of 940 mL volume. The procedure was conducted at 11 ± 1 MPa and 60 °C, by using a step procedure involving 5 min ethanol extraction with a flow of CO_2 ($120\text{--}160$ g min^{-1}) followed by 30 min during which the CO_2 flow was decreased to 0 g min^{-1} to allow the balancing of ethanol between pea matrix and headspace. This procedure was repeated 4 times before final depressurization in 30 min.

AD, FD, and SE + SCD pea powders were ground using a lab grinder (8010 EB, Warning Commercial, Torrington, Connecticut) for 5 min and stored at 20 °C in sealed plastic bags until use.

2.2. Composition

Chemical composition of blanched green peas were analyzed by the reference AOAC method. Soluble and insoluble dietary fiber were analyzed according to AOAC method using a total dietary fiber assay kit (TDF-100A, Sigma-Aldrich, St. Louis, Missouri, USA) (AOAC, 2011). Moisture content was calculated according to AOAC gravimetric method (AOAC, 2005a). Total proteins were calculated according to Kjeldahl method (AOAC, 2005b). Total lipids were determined according to Soxhlet extraction with diethyl ether (AOAC, 2005c). The amount of ash was calculated by incineration of around 10 g of sample using the muffle (RO-8, Gossen Metrawatt, Nürnberg, Germany) (AOAC, 1923).

2.3. Fourier transform infrared spectroscopy (FTIR)

The FTIR spectra were acquired by a Bruker Tensor 27 (Bruker Optik GmbH, Ettlingen, Germany) equipped with Attenuated Total Reflectance (ATR) cell (Pike Technology Inc., Madison, WI, USA). The powders were placed on the FTIR sample holder and pressed with a flat-tipped plunger to obtain suitable spectral peaks. OPUS 7.5 software (Bruker Optik GmbH, Ettlingen, Germany) was used to record the spectra from 900 to 4000 cm^{-1} with an average of 120 scans at a resolution of 4 cm^{-1} . The background was scanned before each sample scanning. Atmosphere compensation (H_2O and CO_2 compensations) and vector normalization were conducted by OPUS 7.5 (version 7.0 for Microsoft Windows, Bruker Optics, Milan, Italy). OriginPro 2021 (OriginLab, Northampton, MA, USA) was used for data plotting and peaks' deconvolution and fitting. Hidden peaks were searched using a second derivative method with smoothing using a 5-point Savitsky-Golay function. The spectra range of amide I was fitted with Gaussian band profile in the OriginPro (version 2021, OriginLab Corporation, Northampton, MA, USA) and the amount of each secondary structure was calculated as the percentage of each fitted area to the total peak area. The fitting quality of the Gaussian curves was confirmed by having $R^2 > 0.997$.

2.4. Image acquisition

Images were acquired using an image acquisition cabinet (Immagini & Computer, Bareggio, Italy) equipped with a digital camera (EOS 550D, Canon, Milan, Italy). The light was provided by 4100 W frosted photographic floodlights. Images were saved in *jpeg* format resulting in 3456×2304 pixels.

2.5. Colour

A tristimulus colorimeter (Chromameter-2 Reflectance, Minolta, Osaka, Japan) equipped with a CR-300 measuring head was used. Petri dishes with a diameter of 90 mm and a height of 16 mm were fully filled with powder. At least 5 measures were taken for each sample. Colour was expressed in CIE L^* , a^* , b^* scale parameters. Colour difference (ΔE) was calculated by the following equation:

$$\Delta E = \sqrt{(L_{FD} - L)^2 + (a_{FD} - a)^2 + (b_{FD} - b)^2} \quad (\text{eq. 1})$$

where L_{FD} , a_{FD} and b_{FD} are the colour parameters of FD sample and L , a , and b are the colour parameters of the AD or SCD samples.

2.6. Bulk density

The bulk density of pea powders was estimated by measuring the volume of a known amount of powder and expressed as g cm^{-3} . To this aim, 2.5 ± 0.1 g of powder was inserted into a graduated syringe and tapped gently.

2.7. Particle size distribution

About 20 g of powder was sieved with a set of sieves with 100, 200, 500, and 1000 μm mesh size (FTS-0200, Filtra Vibracion, Barcelona, Spain). The amount of powder remaining in each sieve was weighed and expressed as a percentage of initial powder weight.

2.8. Scanning electronic microscopy (SEM)

Pea powders were observed by SEM (Zeiss-Supra 40 VP/Gemini Column, Carl Zeiss, Germany) with a built-in light microscope and camera (Instruction BX51, Olympus, Tokyo, Japan). Samples were prepared according to Yanjun et al. (2014) with modification. Double-sided sticky tape was attached to SEM specimen stubs, then a thin layer of powder was spreaded uniformly on the tape and sputter-coated with gold in K575X sputter coater (K575X Sputter Coater, Quorum Technologies, UK). After the specimen stubs were placed at the proper position in the observation room, coated samples were examined at an accelerator voltage of 15 kV. Images were taken at magnifications of $200 \times$ and $500 \times$ times. At least 10 images were recorded for each sample and the most representative one was chosen.

2.9. Wettability

Optical tensiometer (Attention Theta, Biolin Scientific Ltd., Espoo, Finland) with built-in high-speed camera was used to monitor the wetting of powders according to sessile drop spread wetting procedure reported by Ji, Fitzpatrick, Cronin, Crean, and Miao (2016) with some modifications. The liquid droplet standing on the surface of samples was allowed to be naturally absorbed into the solid phase without external forces. Three grams of powder was loaded in the containers and gently pressed 5 times by a flat spatula to form a smooth surface; a set volume of 12 mL deionized water was dropped down and onto the surface of the powder at room temperature. The images of the water droplet remaining above the powder as a function of time (totally 300 s) were recorded. Wetting time was defined as the time at which the water droplet was no more visible on the powder surface. Measurements for each sample were repeated 5 times.

2.10. Solubility

Two grams of water at ambient temperature was added to 0.04 g (W_0) powder samples into a tared 2-mL Eppendorf tube, mixed with a vortex (Vortex 1, Ika, Milan, Italy) 4 times for 30 s and left overnight at 4 °C to allow solubilization. The solutions were centrifuged 20 min (Mikro 20, Hettich Zentrifugen, Tuttlingen, Germany) at $20,000 \times g$ at 4 °C. The supernatant was eliminated, and the sediment was dried overnight at 75 °C under vacuum (Vuotomatic 50 B.E. 73, Bicasa, Milano, Italia) and then weighted (W_1). Powder solubility was calculated according to eq. (2):

$$\text{Solubility (\%)} = [1 - W_1 / (W_0 \bullet D.M.)] \bullet 100 \quad (\text{eq. 2})$$

where *D.M.* is the dry matter (g/100 g) of the powders.

2.11. Water and oil holding capacity

An amount of 0.04 g pea powder was inserted into pre-weighed tared 2-mL Eppendorf tubes and added with 1 mL distilled water or sunflower oil. The tubes were stirred using a vortex (Vortex 1, Ika, Milan, Italy) for 20 s and centrifuged 20 min at 20,000×g at 4 °C (Mikro 20, Hettich-Zentrifugen, Tuttlingen, Germany). The resulting supernatant was carefully removed and the sediment was weighed. Water (WHC) and oil holding capacity (OHC) were expressed as g of water or oil held per g of powder.

2.12. Sensory analysis

Twenty judges, with previous experience in sensory analysis, were recruited among students and workers at the University of Udine. Judges were informed of the details of the study and the risks involved in the participation. Smoking, eating, or drinking was forbidden for at least 1 h before the sensory tests. The sessions were performed between 9:00 and 11:00 a.m. in a sensory laboratory equipped according to the UNI-EN ISO 8589 regulation for food sensory evaluation. The sensory properties of pea powders were assessed based on 3 descriptors selected based on the literature (Cosson et al., 2020). The evaluated descriptors were texture graininess, vegetal flavor, and pea flavor. The descriptors were discussed among the judges and shared definitions were determined through consensus. Following, pea powders (0.7 g), identified with a three-digit random code, were provided to the judges, who were asked to eat the samples and evaluate the intensity of the descriptors by using a 3-point scale (not perceptible, moderate, strong). Water was used to rinse the mouth among the samples. The study complied with the principles established by the Declaration of Helsinki and the protocol was approved by the Institutional Review Board of the Department of Agricultural, Food, Environmental and Animal Sciences of the University of Udine (protocol n. 0002511).

2.13. Data analysis

If not specified, analyses were carried out at least three times in two replicated experiments. Analysis of variance (ANOVA) and significance of mean differences, assessed through Tukey's test ($p < 0.05$), were performed using R (The R foundation for statistical computing, v.3.1.1).

3. Results and discussion

3.1. Chemical properties

Table 1 shows the chemical composition of pea powders obtained via air-drying (AD), freeze-drying (FD), and solvent exchange followed by supercritical- CO_2 -drying (SE + SCD). Independently of the drying technique, powders rich in insoluble fibers (from 28.16 to 30.77 g/100 g), carbohydrates (from 27.17 to 37.17 g/100 g), and proteins (from 23.77 to 31.55 g/100 g) were obtained. Nevertheless, the application of SE + SCD resulted in a significant reduction of the carbohydrate (17.79 % less than AD and 26.90 % less than FD) and lipid (95.83 % less than

AD and 96.05 % less than FD) content with a consequent increase of the protein and fiber fractions in the powder. Low molecular weight pea carbohydrates were probably solubilized during solvent exchange from water to ethanol. SE + SCD technique is also known to promote the removal of lipidic compounds from the treated matrix during both SE and SCD (Konak et al., 2014).

Besides composition, the drying technique might also affect the conformation of pea components and their interactions. For these reasons, FTIR analysis was conducted (Fig. 1). All pea powders revealed a broad peak around 3300 cm^{-1} , related to the absorption of O–H stretching, associated with the hydrogen-bonded hydroxyl groups, probably due to the presence of water molecules in the pea powders (Table 1). The absorption of this band was comparable in all samples, despite the higher moisture content of the SE + SCD sample. Also the peaks observed at 1047 cm^{-1} , assigned to crystalline starch (Vatanev et al., 2021), resulted unaffected by the drying technique. Conversely, a peak at 2846 cm^{-1} , assigned to the C–H stretching and bending vibration in hemicellulose (Arthanarieswaran, Kumaravel, & Saravanakumar, 2015), was observed in AD and FD samples, but not in the SE + SCD powder. Since hemicellulose is precipitated by ethanol, the water-to-ethanol SE prior to SCD probably caused a reduction in the structural mobility of hemicellulose (Arthanarieswaran et al., 2015). Considering the signals associated with lipids, two distinctive peaks were found at 2928 cm^{-1} (H–C–H stretching in lipid acyl chains) and 1741 cm^{-1} (ester C=O stretching) in AD and FD powders, but not in the SE + SCD (Ami et al., 2014). This result confirms compositional data reported in Table 1 and the lipid-extracting effect of SE + SCD (Barry, Dinan, & Kelly, 2017). Finally, an intense peak in the range from 1600 to 1700 cm^{-1} was detected in all FTIR spectra, corresponding to Amide I, which is one of fingerprint regions relevant to proteins. Peak deconvolution and fitting were conducted to quantify protein secondary structures (Fig. S1), including intermolecular β -sheet (1610–1627 cm^{-1}),

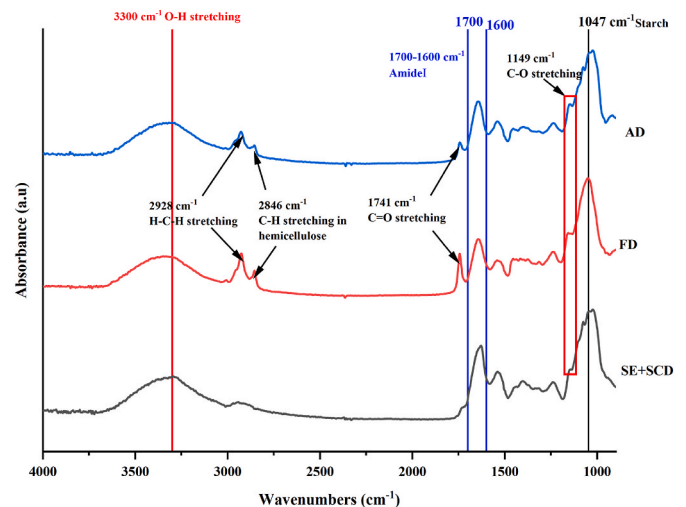


Fig. 1. ATR-FTIR spectra (4000–900 cm^{-1}) of pea powders obtained via air-drying (AD), freeze-drying (FD) and solvent exchange followed by supercritical- CO_2 -drying (SE + SCD).

Table 1

Moisture, lipid, protein, fiber, carbohydrate, and ash content (g/100 g powder) of pea powders obtained via air-drying (AD), freeze-drying (FD) and solvent exchange followed by supercritical- CO_2 -drying (SE + SCD).

Drying technique	Moisture	Carbohydrates	Proteins	Lipids	Unsoluble fibers	Soluble fibres	Ashes
AD	6.77 ± 0.01 ^b	33.05 ± 0.71 ^b	23.80 ± 0.15 ^b	2.40 ± 0.20 ^a	30.77 ± 0.35 ^{ab}	0.09 ± 0.01 ^a	3.12 ± 0.01 ^a
FD	5.14 ± 0.06 ^c	37.17 ± 1.23 ^a	23.77 ± 0.42 ^b	2.53 ± 0.08 ^a	28.16 ± 0.63 ^b	0.06 ± 0.01 ^b	3.17 ± 0.03 ^a
SE + SCD	7.96 ± 0.08 ^a	27.17 ± 1.09 ^c	31.55 ± 0.22 ^a	0.10 ± 0.01 ^b	29.82 ± 0.76 ^a	0.04 ± 0.01 ^b	3.27 ± 0.01 ^a

^{a,b,c}: in the same column, means indicated by different letters are significantly different ($p < 0.05$).

Values are mean ($n = 6$) ± standard deviation.

β -sheet (1628–1642 cm^{-1}), random coil (1643–1650 cm^{-1}), and β -turn (1660–1699 cm^{-1}) (Dong, Huang, & Caughey, 1990; Ngarize, Herman, Adams, & Howell, 2004; Sadat & Joye, 2020). The fitting results and the relative proportion of proteins secondary structured are shown in Fig. 2. All the samples presented a relatively high amount of β -structure (β -turn and β -sheet), in agreement with the literature. In particular, according to the study of Lan, Xu, Ohm, Chen, and Rao (2019), the predominant secondary structure of pea proteins is β -sheet, which is commonly found in the hydrophobic core of folded proteins. AD significantly decreased the β -sheet structure as compared to FD, while in SE + SCD samples its content was higher. Moreover, most β -sheet structure in AD samples (31.07 %) was represented by intermolecular arrangements, while in SE + SCD samples a larger amount of non-intermolecular β -sheet structures were detected (77.08 %). Random coil structure was not detected in SE + SCD samples, while its proportion increased after AD treatment in comparison to FD.

Overall, these results indicate that SE + SCD probably led to the formation of insoluble protein aggregates. It is well known that the polarity of the environment progressively decreases during SE and SCD, promoting protein-protein interaction (Ganesan et al., 2018). Moreover, supercritical CO_2 was reported to be able to induce modifications of the secondary and tertiary structure of proteins by favouring the exposure of hydrophobic groups resulting in their interaction (Manzocco et al., 2021; Xu et al., 2011).

3.2. Physical properties

The drying technique strongly affected the colour of the powders (Table 2). The FD powder presented a bright green colour, with the lowest a^* (-18.5 ± 0.1) and the highest b^* value (35.2 ± 0.4), indicating that, as expected, FD preserved the original pea waste colour, due to the mild temperature conditions applied (Adam, Mühlbauer, Esper, Wolf, & Spiess, 2000). By contrast, the AD sample appeared more brownish as compared to the FD sample, due to the thermal degradation of pea pigments (Zielinska, Zapotoczny, Alves-Filho, Eikevik, & Blaszcak, 2013). The different effect of AD as compared to FD on the colour of pea powders was also estimated by calculating the ΔE value, which resulted of 14.3 ± 2.9 (Table 2). Interestingly, the SE + SCD powder appeared bleached, with the highest luminosity ($L^* = 92.0 \pm 0.8$) value and a^* and b^* values approaching the achromatic point (-1.9 ± 0.1 and 8.7 ± 0.6 , respectively). The strong variation of pea colour

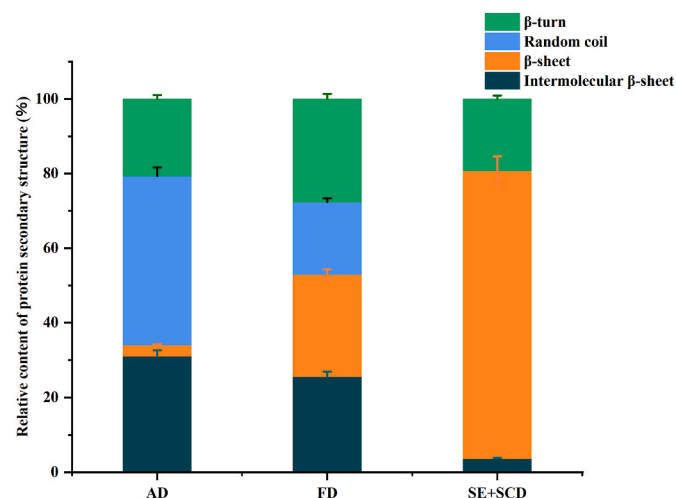


Fig. 2. Relative proportion of protein secondary structure calculated from ATR-FTIR spectra in the Amide I ($1700\text{--}1600\text{ cm}^{-1}$) region of pea powders obtained via air-drying (AD), freeze-drying (FD) and solvent exchange followed by supercritical- CO_2 -drying (SE + SCD). Values are mean ($n = 6$) \pm standard deviation.

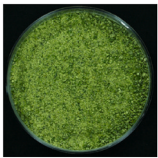


upon SE + SCD was confirmed by the high ΔE value (34.4 ± 1.5). Such results are attributable to pea pigment extraction, extensively occurring during the SE. In particular, chlorophylls are highly soluble in ethanol (Macías-Sánchez et al., 2008).

The AD powder presented a bulk density ($0.830 \pm 0.019\text{ g cm}^{-3}$) more than double as compared to the FD powder ($0.375 \pm 0.030\text{ g cm}^{-3}$), probably due to the severe structural collapse caused by water evaporation (Table 2). By contrast, the SE + SCD powder presented the lowest bulk density ($0.162 \pm 0.006\text{ g cm}^{-3}$), which can be attributed to tissue expansion during the decompression of the SCD reactor (Brown et al., 2008; Plazzotta et al., 2018b). To confirm the effect of the drying technique on pea powder structure, the microstructural features of the samples were analyzed by SEM (Fig. 3). In all cases, the powder microstructure appeared composed by a porous fibrous matrix embedding the other pea compounds. At higher magnification, starch granules (red arrows), with the typical spheroidal shape with a $10\text{--}45\text{ }\mu\text{m}$ diameter (Jane, Kasemsuwan, Leas, Zobel, & Robyt, 1994), and protein fragments (red circles) were identified in all samples. The original cellular organization was no longer evident in the AD powder microstructure, which presented large collapsed aggregates, formed upon the intense capillary tensions suffered by the pea tissue during water evaporation (Ahmed, Sorifa, & Eun, 2010). The original tissue structure was instead recognized in the FD sample micrograph, along with extended sheet-like areas, probably formed during local tissue collapse induced by ice crystal growth (Bhatta, Janezic, & Ratti, 2020). The latter was responsible for the formation of large and not-homogeneously distributed pores, most of them being closed upon the local collapse of cellular material induced by the ballooning effect of ice crystals (Fig. 3). The typical microstructure of vegetable cellular tissues was well-evident also in the SE + SCD sample micrograph. The SCD-dried cell scaffolds appeared as a homogeneous honeycomb with walls formed by irregular fiber structures. As a result, a fine open porosity, corresponding to the voids left by cellular content, was observed. Similar effects were also reported upon ethanol-aided SCD of carrot slices and SE + SCD applied to lettuce leaves (Brown et al., 2008; Plazzotta et al., 2018a; Plazzotta et al., 2018a). The ability of SE + SCD to maintain cellular organization is related to the absence of capillary forces during ethanol extraction with supercritical- CO_2 , and to tissue expansion during the last stages of SCD, in which pressurized CO_2 is released. Such microstructural evidence demonstrates the ability of SE + SCD to better maintain the original tissue structure as compared to AD and FD, leading to an aerated low-density powder (Table 2) with a high void volume organised in homogeneous open pores (Fig. 3).

The observed differences in the microstructure (Fig. 3) and density (Table 2) upon different drying techniques also resulted in powders with different granulometry (Fig. 4). All pea powders presented most particles in the range $200\text{--}1000\text{ }\mu\text{m}$. The AD and SE + SCD powders presented a comparable particle size distribution, with most particles (about 45 %) in the range $500\text{--}1000\text{ }\mu\text{m}$, followed by the family in the dimension range $200\text{--}500\text{ }\mu\text{m}$ (about 30 %). The remaining particle fraction was evenly distributed in the family ranges $>1000\text{ }\mu\text{m}$, $100\text{--}200\text{ }\mu\text{m}$ and $<100\text{ }\mu\text{m}$. By contrast, the FD powder presented a more homogeneous particle size distribution, with about 70 % of the particles in the $200\text{--}500\text{ }\mu\text{m}$ dimension range, and only a minor particle fraction $>500\text{ }\mu\text{m}$. Such results can be traced back to the propensity of dried materials with different physico-chemical properties to undergo breaking during grinding. In particular, AD produced large collapsed particles (Fig. 3) presenting a hard texture, difficult to downsize. A similar low propensity to particle downsizing was also observed in the SE + SCD powder, despite its aerated structure (Fig. 3). It can be inferred that protein conformational changes upon SE + SCD (Fig. 2) may have induced the formation of protein aggregates, physically embedding the other pea compounds. Such aggregates of components would intimately interact at both chemical and physical level, opposing downsizing. Moreover, it cannot be excluded that the low density of the SE + SCD powder (Table 2) affected the grinding behaviour by modifying powder

Table 2

Appearance, colorimetric parameters (L^* , a^* , b^*), colour difference (ΔE) and bulk density of pea powders obtained via air-drying (AD), freeze-drying (FD) and solvent exchange followed by supercritical- CO_2 -drying (SE + SCD).

Drying technique	Appearance	L^*	a^*	b^*	ΔE	Bulk density (g cm^{-3})
AD		67.6 ± 1.8^c	-13.5 ± 0.6^b	26.4 ± 1.1^a	14.3 ± 2.9	0.830 ± 0.019^a
FD		77.7 ± 0.7^b	-18.5 ± 0.1^c	35.2 ± 0.4^b	Control*	0.375 ± 0.030^b
SE + SCD		92.0 ± 0.8^a	-1.9 ± 0.1^a	8.7 ± 0.6^c	34.4 ± 1.5	0.162 ± 0.006^c

^{a,b,c}: in the same column, means indicated by different letters are significantly different ($p < 0.05$).

Values are mean ($n = 6$) \pm standard deviation. * ΔE was expressed considering the FD pea powder as the control (see section 2.5 in Materials and Methods).

flow pattern in the grinder (Chao, Wang, Jakobsen, Fernandino, & Jakobsen, 2012).

3.3. Interaction with water and oil

The chemical and structural differences among pea powders are expected to modify their ability to interact with food fluids. Fig. 5 reports the images of water droplets on top of the different pea powders as a function of time as an indication of powder wettability. In all cases, upon contact with the powder surface, the water droplet was progressively absorbed by the powder, leading to a progressive disappearance of the typical droplet shape profile over time. For both AD and FD powders, the water droplet was no more evident after 0.86 s, which thus corresponded to their wetting time. By contrast, once the water droplet came into contact with the SE + SCD sample, the pea particles quickly swelled upon fast water uptake, modifying the appearance of the water-air interface of the droplet. The droplet showed a rough surface, which was well-evident (red circles) even after 2.72 s of contact (Fig. 5). This peculiar effect can be attributed to the structural organization of SE + SCD particles which were characterized by a homogeneous distribution of a number of small open pores (Fig. 3), exerting strong capillary forces driving water uptake into them (Zou et al., 2023). By contrast, capillary forces were much lower in AD or FD powders, which were highly collapsed or presented larger and partially closed pores, respectively. In these cases, water was mainly absorbed in the interstices among particles without causing their swelling (Zheng et al., 2020). These results agree with the fact that SE + SCD powder presented a lower solubility (13.6 ± 0.7 g/100 g) than AD (33.5 ± 0.9 g/100 g) and FD (36.1 ± 1.2 g/100 g) samples, but a much higher water holding capacity (5.2 ± 0.6 , 2.6 ± 0.3 , and 3.1 ± 0.3 g water/g powder respectively) (Table 3). The low solubility of the SE + SCD samples is likely attributable to: (i) loss of ethanol soluble compounds, mainly carbohydrates and pigments, during the SE phase of the SCD process (Macías-Sánchez et al., 2008); (ii) conformational changes of polysaccharides and proteins upon polarity modifications during SE + SCD (Fig. 1); (iii) denaturation of proteins

caused by the ethanol and interaction among biopolymers (Mekala & Saldaña, 2023). Nevertheless, the highly porous particles generated upon SE + SCD were able to tightly retain the absorbed water into the complex network of pore channels, despite the lower hydrophobicity of their surface. This hypothesis is supported by literature evidences collected on SE + SCD powders obtained from lettuce and on SE + SCD cellulose networks, which presented unexpectedly high WHC (Plazzotta, Ibraz, Manzocco, & Martín-Belloso, 2021a; Ciuffarin et al., 2023).

The physically driven absorption capacity of SE + SCD powder was further confirmed by OHC analysis. The oil amount absorbed by the AD (0.8 ± 0.1 g oil/g powder) and FD (1.5 ± 0.3 g oil/g powder) powders was significantly lower than that of water (Table 3), probably due to the hydrophilic nature of cellular materials exposing onto the pea particles surface. By contrast, SE + SCD powders (4.7 ± 0.9 g oil/g powder) showed comparable WHC and OHC. Large amounts of different solvents would be easily uptaken into the small pores of SE + SCD powders, independently of fluid polarity, since mostly driven by capillary forces. This property could have interesting practical relevance, suggesting the possible exploitation of SE + SCD powders as bulking agent in moist food formulations, or as structuring agent for liquid oil.

3.4. Sensory properties

Lastly, the effect of the drying technique on pea powder sensory attributes was evaluated. Fig. 6 reports the percentage of judges that, upon tasting the pea powders, evaluated graininess, vegetal and pea flavour as not perceptible, moderate, or strong. The AD powder was perceived by more than 90 % of the judges as strongly grainy, probably due to its high-density collapsed structure, formed by large aggregates with dimensions higher than 500 μm (Table 2, Figs. 3, Figure 4). Interestingly, despite the different granulometry (Fig. 4), SE + SCD and FD powders showed comparable graininess scores, indicating powder density (Table 2), rather than particle dimension distribution, to be the main structural feature affecting graininess mouthfeel. As expected, almost all the judges evaluated the FD powder to present a strong

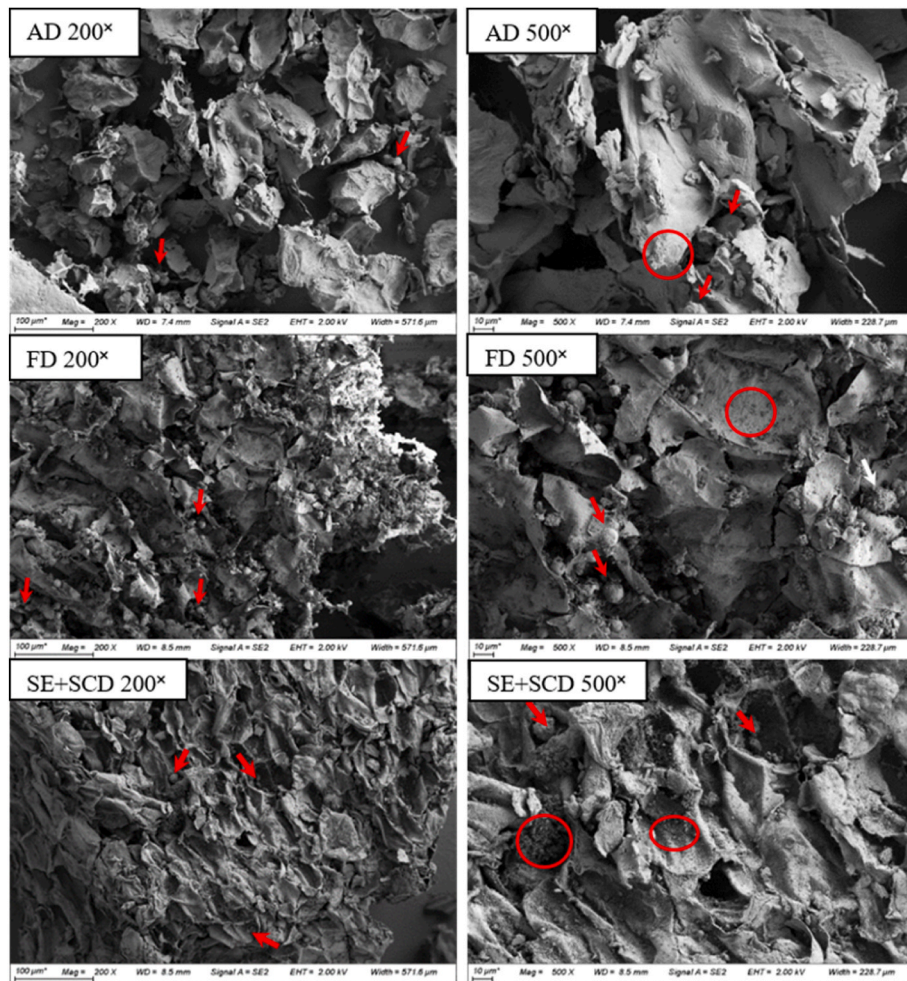


Fig. 3. Scanning electron microscope images with 200* and 500 * magnification of pea powders obtained via air-drying (AD), freeze-drying (FD) and solvent exchange followed by supercritical-CO₂-drying (SE + SCD). Red arrows indicate starch granules; red circles indicate protein fragments. (For interpretation of the references to colour in this figure legend, the reader is referred to the Web version of this article.)

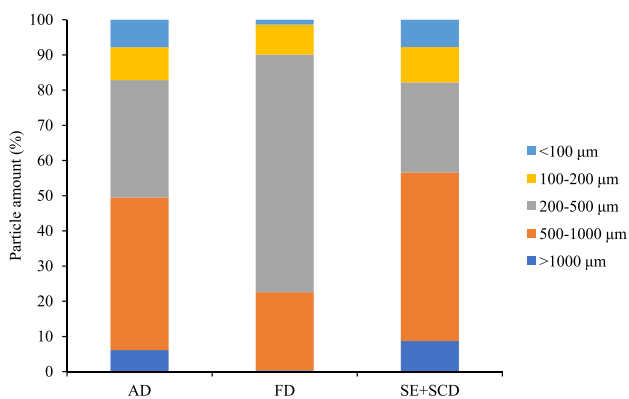


Fig. 4. Particle size distribution (%) of pea powders obtained via air-drying (AD), freeze-drying (FD) and solvent exchange followed by supercritical-CO₂-drying (SE + SCD).

vegetal and pea flavor (Fig. 6). Thanks to the mild temperature conditions applied during FD, this technique led to a powder highly preserving the sensory flavor of the fresh peas. These vegetable and pea flavors were instead defined “moderate” by the majority of the judges when evaluating the AD powder. The heat-induced degradation of pea

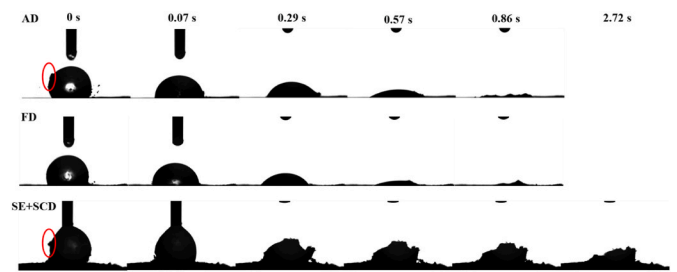


Fig. 5. Images of water droplets above the pea powders obtained via air-drying (AD), freeze-drying (FD) and solvent exchange followed by supercritical-CO₂-drying (SE + SCD) as a function of time. Red circles represent pea powders attaching on the surface of water droplets. (For interpretation of the references to colour in this figure legend, the reader is referred to the Web version of this article.)

compounds during AD are well-known to induce significant changes in the sensory profile of vegetable powders (Trindler, Annika Kopf-Bolanz, & Denkel, 2022). More than 80 % of the judges was not able to perceive the vegetable flavor in the SE + SCD powder, and no one of them perceived pea flavor. This is likely due to the loss of most of the compounds responsible for pea flavor during SE and SCD (Vatansver et al., 2020, 2021, 2022). In this regard, the typical pea flavor is related to the presence of alcohols and aldehydes (Vatansver et al., 2021) which are

Table 3

Solubility, water, and oil holding capacity (WHC and OHC) of pea powders obtained via air-drying (AD), freeze-drying (FD) and solvent exchange followed by supercritical-CO₂-drying (SE + SCD).

Drying technique	Solubility (w/w)	WHC (g water/g powder)	OHC (g oil/g powder)
AD	33.5 ± 0.9 ^a	2.6 ± 0.3 ^c	0.8 ± 0.1 ^c
FD	36.1 ± 1.2 ^a	3.1 ± 0.3 ^b	1.5 ± 0.3 ^b
SE + SCD	13.6 ± 0.7 ^b	5.2 ± 0.6 ^a	4.7 ± 0.9 ^a

^{a,b,c}: in the same column, means indicated by different letters are significantly different ($p < 0.05$).

Values are mean ($n = 6$) ± standard deviation.

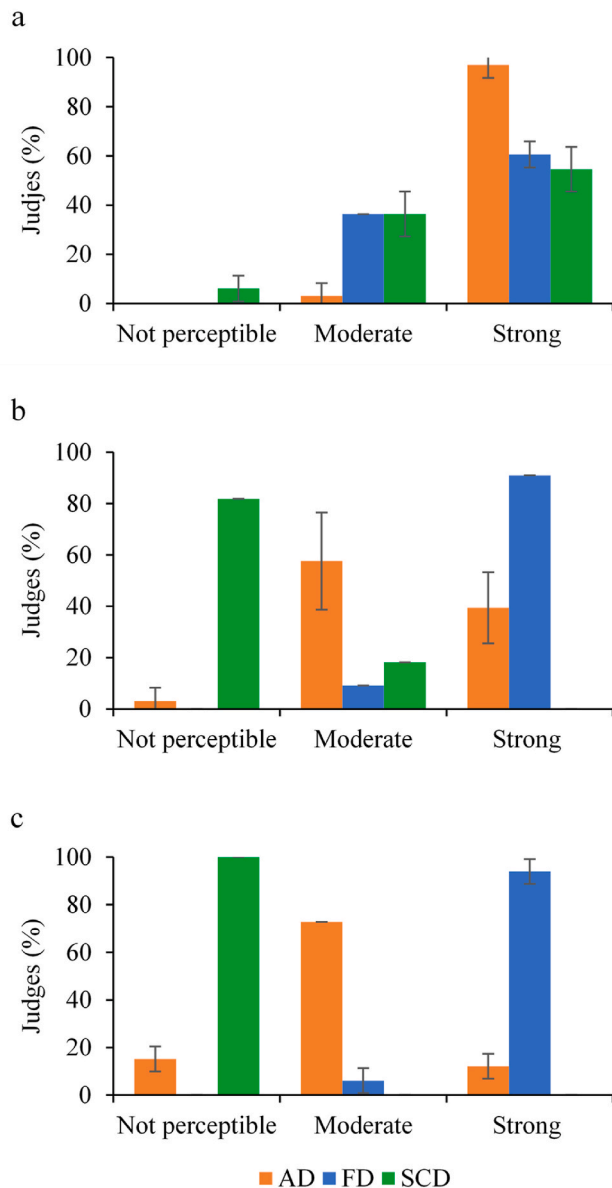


Fig. 6. Percentage of judges that recognized perceptible, moderate or strong intensity of graininess (a), vegetal (b) and pea flavour (c) in pea powders obtained via air-drying (AD), freeze-drying (FD) and solvent exchange followed by supercritical-CO₂-drying (SE + SCD). Values are mean ($n = 3$) ± standard deviation.

well-solubilized in both hydroalcoholic solutions and in supercritical CO₂. These results show that SE + SCD produced a flavorless material, with no vegetable sensory notes. This makes SE + SCD powders a particularly interesting ingredient, potentially exploitable in the formulation of a wide variety of food products without altering their sensory acceptability.

4. Conclusions

Results of this study demonstrate the feasibility of using SCD associated with water-to-ethanol SE as valuable strategy to convert sub-standard peas into innovative food ingredients with target technological and sensory properties. This technology allows obtaining a pea powder with excellent rehydration ability and oil absorption capacity, owing to its low density and highly porous microstructure, along with biopolymer conformational changes. Also, the SE + SCD powder resulted colourless, tasteless and flavourless, losing the typical sensory attributes of green peas, which are undesired for many food applications. These peculiar technological and sensory functionalities could facilitate the exploitation of this high-protein, high-fiber powder as a food ingredient. Nevertheless, further research activities are needed to better understand the performances of SE + SCD pea powder in complex food formulations. Moreover, the ethanolic extract remaining after the SE step of the SE + SCD procedure could be further processed in order to isolate the pea valuable pea compounds (e.g., chlorophylls and polyphenols) extracted in this stage, accomplishing a zero-waste upcycling of discarded peas. Finally, the proposed approach could be also used to valorize wastes generated from pulses other than peas, such as soy, lentils and beans.

Funding

This research did not receive any specific grant from funding agencies in the public, commercial, or not-for-profit sectors.

CRediT authorship contribution statement

Lara Manzocco: Conceptualization, Project administration, Resources, Supervision, Writing – review & editing. **Lorenzo Barozzi:** Data curation, Formal analysis, Investigation, Methodology, Visualization, Writing – original draft, Writing – review & editing. **Stella Plazzotta:** Conceptualization, Methodology, Visualization, Writing – review & editing. **Yanjun Sun:** Data curation, Formal analysis, Investigation, Methodology, Writing – review & editing. **Song Miao:** Resources, Supervision, Writing – review & editing. **Sonia Calligaris:** Conceptualization, Project administration, Resources, Writing – review & editing.

Declaration of competing interest

The authors declare that they have no known competing financial interests or personal relationships that could have appeared to influence the work reported in this paper.

Data availability

Data will be made available on request.

Acknowledgments

This work was supported by the University of Udine in the framework of the Strategic Plan 2022–2025, Interdepartmental Research Project CibiAmo.

Appendix A. Supplementary data

Supplementary data to this article can be found online at <https://doi.org/10.1016/j.lwt.2024.115778>.

[org/10.1016/j.lwt.2024.115778](https://doi.org/10.1016/j.lwt.2024.115778).

References

- Adam, E., Mühlbauer, W., Esper, A., Wolf, W., & Spiess, W. (2000). Quality changes of onion (*Allium cepa* L.) as affected by the drying process. *Nahrung-Food*, *44*, 32–37. [https://doi.org/10.1002/\(sici\)1521-3803\(20000101\)44:1<32::aid-food32>3.0.co;2-f](https://doi.org/10.1002/(sici)1521-3803(20000101)44:1<32::aid-food32>3.0.co;2-f)
- Ahmed, M., Sorifa, A. M., & Eun, J. B. (2010). Effect of pretreatments and drying temperatures on sweet potato flour. *International Journal of Food Science and Technology*, *45*, 726–732. <https://doi.org/10.1111/j.1365-2621.2010.02191.x>
- Akharume, F. U., Aluko, R. E., & Adedeji, A. A. (2021). Modification of plant proteins for improved functionality: A review. *Comprehensive Reviews in Food Science and Food Safety*, *20*, 198–224. <https://doi.org/10.1111/1541-4337.12688>
- Ami, D., Posteri, R., Mereghetti, P., Porro, D., Doglia, S. M., & Branduardi, P. (2014). Fourier transform infrared spectroscopy as a method to study lipid accumulation in oleaginous yeasts. *Biotechnology for Biofuels*, *7*, 1–14. <https://doi.org/10.1186/1754-6834-7-12>
- AOAC Official Method 2001.11. (2005b). In *Official methods of analysis* (18th ed.). Gaithersburg, MD, USA: AOAC INTERNATIONAL.
- AOAC Official Method 2001.12. (2005c). In *Official methods of analysis* (18th ed.). Gaithersburg, MD, USA: AOAC INTERNATIONAL.
- AOAC Official Method 2003.05. (2005a). In *Official methods of analysis* (18th ed.). Gaithersburg, MD, USA: AOAC INTERNATIONAL.
- AOAC Official Method 2011.25. (2011). In *Official methods of analysis* (18th ed.). Gaithersburg, MD, USA: AOAC INTERNATIONAL.
- AOAC Official Method 923.03. (1923). *Official methods of analysis* (7th ed.). Gaithersburg, MD, USA: AOAC INTERNATIONAL.
- Arthanarieswaran, V. P., Kumaravel, A., & Saravanakumar, S. S. (2015). Characterization of new natural cellulose fiber from *Acacia leucophloea* Bark. *International Journal of Polymer Analysis and Characterization*, *20*, 367–376. <https://doi.org/10.1080/1023666X.2015.1018737>
- Barry, K. M., Dinan, T. G., & Kelly, P. M. (2017). Pilot scale production of a phospholipid-enriched dairy ingredient by means of an optimised integrated process employing enzymatic hydrolysis, ultrafiltration and super-critical fluid extraction. *Innovative Food Science and Emerging Technologies*, *41*, 301–306. <https://doi.org/10.1016/j.ifset.2017.04.004>
- Bhatta, S., Janezic, T. S., & Ratti, C. (2020). Freeze-drying of plant-based foods. *Foods*, *9*, 87. <https://doi.org/10.3390/foods9010087>
- Brown, Z. K., Fryer, P. J., Norton, I. T., Bakalis, S., & Bridson, R. H. (2008). Drying of foods using supercritical carbon dioxide - investigations with carrot. *Innovative Food Science and Emerging Technologies*, *9*, 280–289. <https://doi.org/10.1016/j.ifset.2007.07.003>
- Chao, Z., Wang, Y., Jakobsen, J. P., Fernandez, M., & Jakobsen, H. A. (2012). Multi-fluid modeling of density segregation in a dense binary fluidized bed. *Particology*, *10*, 62–71. <https://doi.org/10.1016/j.partic.2011.10.001>
- Ciuffarin, F., Négrier, M., Plazzotta, S., Liberalato, M., Calligaris, S., Budtova, T., et al. (2023). Interactions of cellulose cryogels and aerogels with water and oil: Structure-function relationships. *Food Hydrocolloids*, *140*, Article 108631. <https://doi.org/10.1016/j.foodhyd.2023.108631>
- Cosson, A., Delarue, J., Mabilhe, A. C., Druon, A., Descamps, N., Roturier, J. M., et al. (2020). Block protocol for conventional profiling to sensory characterize plant protein isolates. *Food Quality and Preference*, *83*, Article 103927. <https://doi.org/10.1016/j.foodqual.2020.103927>
- Dong, A., Huang, P., & Caughey, W. S. (1990). Protein secondary structures in water from second-derivative amide I infrared spectra. *Biochemistry*, *29*(13), 3303–3308. <https://doi.org/10.1021/bi00465a022>
- Esparza, I., Jiménez-Moreno, N., Bimbela, F., Ancín-Azpilicueta, C., & Gandía, L. M. (2020). Fruit and vegetable waste management: Conventional and emerging approaches. *Journal of Environmental Management*, *265*, Article 110510. <https://doi.org/10.1016/j.jenvman.2020.110510>
- FAOSTAT. (2021). *Food and agriculture data*. Available online: <http://www.fao.org/faostat/en/#home>. (Accessed 14 March 2023).
- Ganesan, K., Budtova, T., Ratke, L., Gurikov, P., Baudron, V., Preibisch, I., et al. (2018). Review on the production of polysaccharide aerogel particles. *Materials*, *11*, 2144. <https://doi.org/10.3390/ma11112144>
- García-González, C. A., Camino-Rey, M. C., Alnaief, M., Zetl, C., & Smirnova, I. (2012). Supercritical drying of aerogels using CO₂: Effect of extraction time on the end material textural properties. *The Journal of Supercritical Fluids*, *66*, 297–306. <https://doi.org/10.1016/j.supflu.2012.02.026>
- Jakubczyk, E., & Jaskulska, A. (2021). The effect of freeze-drying on the properties of Polish vegetable soups. *Applied Sciences*, *11*, 654. <https://doi.org/10.3390/app11020654>
- Jane, J.-L., Kasemsuwan, T., Leas, S., Zobel, H., & Robyt, J. F. (1994). Anthology of starch granule morphology by scanning electron microscopy. *Starch - Stärke*, *46*, 121–129. <https://doi.org/10.1002/star.19940460402>
- Ji, J., Fitzpatrick, J., Cronin, K., Crean, A., & Miao, S. (2016). Assessment of measurement characteristics for rehydration of milk protein based powders. *Food Hydrocolloids*, *54*, 151–161. <https://doi.org/10.1016/j.foodhyd.2015.09.027>
- Kaveh, M., Abbaspour-Gilandeh, Y., Fatemi, H., & Chen, G. (2021). Impact of different drying methods on the drying time, energy, and quality of green peas. *Journal of Food Processing and Preservation*, *45*, Article e15503. <https://doi.org/10.1111/jfpp.15503>
- Konak, Ü. I., Ercili-Cura, D., Sibakov, J., Sontag-Strohm, T., Certel, M., & Løponen, J. (2014). CO₂-defatted oats: Solubility, emulsification and foaming properties. *Journal of Cereal Science*, *60*, 37–41. <https://doi.org/10.1016/j.jcs.2014.01.013>
- Kumar, M., Tomar, M., Potkule, J., Punia, S., Dhakane-Lad, J., Singh, S., ... Kennedy, J. F. (2022). Functional characterization of plant-based protein to determine its quality for food applications. *Food Hydrocolloids*, *123*, Article 106986. <https://doi.org/10.1016/j.foodhyd.2021.106986>
- Lan, Y., Xu, M., Ohm, J. B., Chen, B., & Rao, J. (2019). Solid dispersion-based spray-drying improves solubility and mitigates beany flavour of pea protein isolate. *Food Chemistry*, *278*, 655–673. <https://doi.org/10.1016/j.foodchem.2018.11.074>
- Macías-Sánchez, M. D., Serrano, C. M., Rodríguez, M. R., de la Ossa, E. M., Lubián, L. M., & Montero, O. (2008). Extraction of carotenoids and chlorophyll from microalgae with supercritical carbon dioxide and ethanol as cosolvent. *Journal of Separation Science*, *31*, 1352–1362. <https://doi.org/10.1002/jssc.200700503>
- Manzocco, L., Plazzotta, S., Powell, J., de Vries, A., Rousseau, D., & Calligaris, S. (2021). Structural characterisation and sorption capability of whey protein aerogels obtained by freeze-drying or supercritical drying. *Food Hydrocolloids*, *122*, Article 107117. <https://doi.org/10.1016/j.foodhyd.2021.107117>
- Mekala, S., & Saldana, M. D. (2023). Lentil protein concentrate+ pectin gels dried with SC-CO₂: Influence of protein-polysaccharide interactions on the characteristics of aerogels. *The Journal of Supercritical Fluids*, Article 106006.
- Michelino, F., Zambon, A., Vizzotto, M. T., Cozzi, S., & Spilimbergo, S. (2018). High power ultrasound combined with supercritical carbon dioxide for the drying and microbial inactivation of coriander. *Journal of CO₂ Utilization*, *24*, 516–521. <https://doi.org/10.1016/j.jcou.2018.02.010>
- Ngarize, S., Herman, H., Adams, A., & Howell, N. (2004). Comparison of changes in the secondary structure of unheated, heated, and high-pressure-treated β-lactoglobulin and ovalbumin proteins using fourier transform Raman spectroscopy and self-deconvolution. *Journal of Agricultural and Food Chemistry*, *52*(21), 6470–6477. <https://doi.org/10.1021/jf030649y>
- Plazzotta, S., Calligaris, S., & Manzocco, L. (2018a). Application of different drying techniques to fresh-cut salad waste to obtain food ingredients rich in antioxidants and with high solvent loading capacity. *LWT*, *89*, 276–283. <https://doi.org/10.1016/j.lwt.2017.10.056>
- Plazzotta, S., Calligaris, S., & Manzocco, L. (2018b). Innovative bioaerogel-like materials from fresh-cut salad waste via supercritical-CO₂-drying. *Innovative Food Science and Emerging Technologies*, *47*, 485–492. <https://doi.org/10.1016/j.ifset.2018.04.022>
- Plazzotta, S., Ibarz, R., Manzocco, L., & Martín-Belloso, O. (2021). Modelling the recovery of biocompounds from peach waste assisted by pulsed electric fields or thermal treatment. *Journal of Food Engineering*, *290*, Article 110196. <https://doi.org/10.1016/j.jfoodeng.2020.110196>
- Pooja, B. K., Sethi, S., Joshi, A., Varghese, E., Kaur, C., Kumar, R., et al. (2023). Ultrasound-assisted extraction of chlorophyll from pea pod waste: Optimization, kinetics, and stability study. *Food Analytical Methods*, *16*, 1358–1369. <https://doi.org/10.1007/s12161-023-02502-8>
- Pravallika, K., Chakraborty, S., & Singhal, R. S. (2023). Supercritical drying of food products: An insightful review. *Journal of Food Engineering*, *343*, Article 111375. <https://doi.org/10.1016/j.jfoodeng.2022.111375>
- Roland, W. S., Pouvreau, L., Curran, J., van de Velde, F., & de Kok, P. M. (2017). Flavor aspects of pulse ingredients. *Cereal Chemistry*, *94*(1), 58–65. <https://doi.org/10.1094/CHEM-06-16-0161-FI>
- Sadat, A., & Joye, I. J. (2020). Peak fitting applied to fourier transform infrared and Raman spectroscopic analysis of proteins. *Applied Sciences*, *10*(17). <https://doi.org/10.3390/app10175918>
- Strumiłło, C., & Adamiec, J. (1996). Energy and quality aspects of food drying. *Drying Technology*, *14*, 423–448. <https://doi.org/10.1080/07373939608917106>
- Tassoni, A., Tedeschi, T., Zurlini, C., Cigognini, I. M., Petrusan, J. I., Rodríguez, Ó., et al. (2020). State-of-the-art production chains for peas, beans and chickpeas—valorization of agro-industrial residues and applications of derived extracts. *Molecules*, *25*, 1383. <https://doi.org/10.3390/molecules25061383>
- Trindler, C., Annika Kopf-Bolanz, K., & Denkel, C. (2022). Aroma of peas, its constituents and reduction strategies – effects from breeding to processing. *Food Chemistry*, *376*, Article 131892. <https://doi.org/10.1016/j.foodchem.2021.131892>
- USDA. (2015). <https://www.usda.gov/consultedon21/05/23>.
- Vatai, T., Škerget, M., & Knez, Ž. (2009). Extraction of phenolic compounds from elder berry and different grape marc varieties using organic solvents and/or supercritical carbon dioxide. *Journal of Food Engineering*, *90*, 246–254. <https://doi.org/10.1016/j.jfoodeng.2008.06.028>
- Vatansever, S., Ohm, J. B., Simsek, S., & Hall, C. (2022). A novel approach: Supercritical carbon dioxide + ethanol extraction to improve techno-functionalities of pea protein isolate. *Cereal Chemistry*, *99*, 130–143. <https://doi.org/10.1002/cche.10489>
- Vatansever, S., Rao, J., & Hall, C. (2020). Effects of ethanol modified supercritical carbon dioxide extraction and particle size on the physical, chemical, and functional properties of yellow pea flour. *Cereal Chemistry*, *97*, 1133–1147. <https://doi.org/10.1002/cche.10334>
- Vatansever, S., Whitney, K., Ohm, J. B., Simsek, S., & Hall, C. (2021). Physicochemical and multi-scale structural alterations of pea starch induced by supercritical carbon dioxide + ethanol extraction. *Food Chemistry*, *344*, Article 128699. <https://doi.org/10.1016/j.foodchem.2020.128699>
- Viganó, J., Machado, A. P. D. F., & Martínez, J. (2015). Sub- and supercritical fluid technology applied to food waste processing. *The Journal of Supercritical Fluids*, *96*, 272–286. <https://doi.org/10.1016/j.supflu.2014.09.026>
- Wouters, A. G., Rombouts, I., Fierens, E., Brijs, K., & Delcour, J. A. (2016). Relevance of the functional properties of enzymatic plant protein hydrolysates in food systems. *Comprehensive Reviews in Food Science and Food Safety*, *15*(4), 786–800. <https://doi.org/10.1111/1541-4337.12209>

- Xu, D., Yuan, F., Jiang, J., Wang, X., Hou, Z., & Gao, Y. (2011). Structural and conformational modification of whey proteins induced by supercritical carbon dioxide. *Innovative Food Science and Emerging Technologies*, 12, 32–37. <https://doi.org/10.1016/j.ifset.2010.10.001>
- Yanjun, S., Jianhang, C., Shuwen, Z., Hongjuan, L., Jing, L., Lu, L., ... Jiaping, L. (2014). Effect of power ultrasound pre-treatment on the physical and functional properties of reconstituted milk protein concentrate. *Journal of Food Engineering*, 124, 11–18. <https://doi.org/10.1016/j.jfoodeng.2013.09.013>
- Zambon, A., Bourdoux, S., Pantano, M. F., Pugno, N. M., Boldrin, F., Hofland, G., et al. (2021). Supercritical CO₂ for the drying and microbial inactivation of apple's slices. *Drying Technology*, 39, 259–267. <https://doi.org/10.1080/07373937.2019.1676774>
- Zambon, A., Zulli, R., Boldrin, F., & Spilimbergo, S. (2022). Microbial inactivation and drying of strawberry slices by supercritical CO₂. *The Journal of Supercritical Fluids*, 180, Article 105430. <https://doi.org/10.1016/j.supflu.2021.105430>
- Zheng, Q., Tian, Y., Ye, F., Zhou, Y., & Zhao, G. (2020). Fabrication and application of starch-based aerogel: Technical strategies. *Trends in Food Science and Technology*, 99, 608–620. <https://doi.org/10.1016/j.tifs.2020.03.038>
- Zia, M., Ahmed, S., & Kumar, A. (2022). Anaerobic digestion (AD) of fruit and vegetable market waste (FVMW): Potential of FVMW, bioreactor performance, co-substrates, and pre-treatment techniques. *Biomass Conversion and Biorefinery*, 12, 3573–3592. <https://doi.org/10.1007/s13399-020-00979-5>
- Zielinska, M., Zapotoczny, P., Alves-Filho, O., Eikevik, T. M., & Blaszcak, W. (2013). Microwave vacuum-assisted drying of green peas using heat pump and fluidized bed: A comparative study between atmospheric freeze drying and hot air convective drying. *Drying Technology*, 31, 633–642. <https://doi.org/10.1080/07373937.2012.751921>
- Zou, Y., Zhang, A., Lin, L., El-Sohaimy, S. A., Li, Y., Wu, L., et al. (2023). Schiff base cross-linked dialdehyde cellulose/gelatin composite aerogels as porous structure templates for oleogels preparation. *International Journal of Biological Macromolecules*, 224, 667–675.